IDŐJÁRÁS

Quarterly Journal of the Hungarian Meteorological Service
Vol. 119, No. 3, July – September, 2015, pp. 307–335

Measuring and modeling of hazardous weather phenomena to aviation using the Hungarian Unmanned Meteorological Aircraft System (HUMAS)

Zsolt Bottyán[1*], **András Zénó Gyöngyösi**[2], **Ferenc Wantuch**[3], **Zoltán Tuba**[1], **Rita Kurunczi**[4], **Péter Kardos**[5], **Zoltán Istenes**[6], **Tamás Weidinger**[2], **Katalin Hadobács**[7], **Zoltán Szabó**[2], **Márton Balczó**[8], **Árpád Varga**[8], **Andrea Bíróné Kircsi**[9], and **Gyula Horváth**[10]

[1]*Department of Military Aviation, National University of Public Service, P. O. Box. 1,H-5008 Szolnok, Hungary*

[2]*Department of Meteorology, Eötvös Loránd University, Pázmány Péter sétány 1/A., H-1117 Budapest, Hungary*

[3]*Aviation Authority, National Transport Authority, Lincoln u. 1., H-2220 Vecsés, Hungary*

[4]*Időkep Ltd., Bartók B. út 65/b., H-1224 Budapest, Hungary*

[5]*HungaroControl, Hungarian Air Navigation Plc, Iglo u. 33–35, H-1185 Budapest, Hungary*

[6]*Department of Software Technology and Methodology, Eötvös Loránd University, Pázmány Péter sétány 1/C., H-1117 Budapest, Hungary*

[7]*Geoinformation Service, Hungarian Defence Forces, H-1524 Budapest, Hungary*

[8]*Department of Fluid Mechanics, Budapest University of Technology and Economics, Budafoki út 8, H-1111 Budapest, Hungary*

[9]*Department of Meteorology, University of Debrecen, H-4032 Debrecen, Egyetem tér 1., Hungary*

[10]*Hungarian Meteorological Service, Gilice tér 39, 1181 Budapest, Hungary*

**Corresponding author E-mail: bottyan.zsolt@uni-nke.hu*

(Manuscript received in final form November18, 2014)

Abstract—At present, Unmanned Aircraft Systems (UAS) are playing more and more significant role in military and civil operations in Hungary. A well-used meteorological support system is essential during the planning and executing phases of different UAS

missions. In the present work, the structure of an applied analog statistical and a WRF-based numerical forecast system is to be introduced with special regards to aviation meteorological factors, such as visibility, ceiling, turbulence, icing, etc. Within such a system, it is very important to generate an accurate short-time visibility prediction. In order to develop such forecasts, we combined an analogy based statistical approach to a high-resolution numerical model for visibility prediction, which are currently available as a hybrid visibility prediction for the regions of four main airports in Hungary. On the other hand, we also present the first Hungarian Unmanned Meteorological Aircraft System (HUMAS). In our case study, the HUMAS measurements are compared to dynamical weather prediction data during the international planetary boundary layer (PBL) campaign in Szeged, Hungary.

Key-words: aviation meteorology, Unmanned Aircraft Systems, integrated forecast system, fuzzy logic, WRF model, visibility, cloud ceiling

1. Introduction

Application of Unmanned Aircraft Systems (UAS) for both civilian and military purposes spreads very rapidly worldwide because of its low operational costs that are expected to even more decrease significantly in the near future (*Gertler*, 2012; *Watts*, 2012). Unmanned systems are playing more and more significant role in military and civil operations also in Hungary (*Fekete* and *Palik*, 2012; *Somlyai et al*., 2012; *Restás*, 2013). Aerial support for natural or industrial disaster management, monitoring (earthquakes, floods and forest fire etc.), government and private survey (cartography, agriculture, wild life monitoring, border control, security and maintenance control for industrial companies, electricity cords or oil and gas pipeline networks, etc.) and the defense of critical infrastructures may benefit from the onboard instruments that might be the payload of such UASs (*Adams* and *Friedland*, 2011; *Gyöngyösi et al.*, 2013; *Restás* and *Dudás*, 2013). Unmanned aviation, on the other hand, is even more sensitive to the actual weather situation than manned flights. Due to their smaller dimensions compared to manned vehicles, the areodynamic processes during flight that highly depend on the present state of the atmosphere are affecting the reliability of flight in a manner more sensitive than for larger sized aircrafts. In addition, the weather itself is able to modify not only the (aero)dynamic aspects of aviation processes but the navigation and execution of a given mission (reconnaissance, observation, etc.), too. The mentioned atmospheric influence on the aviation is more important in the case of unmanned flights which are controlled by autonomous onboard robotic systems or remote pilots (*Williams*, 2004; *Drury et al.*, 2006). These airplanes usually have relatively large wings with a slim airfoil and significant surface area, thus, they are especially sensitive to gusts, turbulence, and airframe icing as well. Beyond that – similarly to manned ones –, they are also sensitive to heavy precipitation, low cloud, and poor visibility condition during their flights (*Østbø et al.*, 2004; *Hadobács et al.*, 2013).

In spite of the relative ease of controlling of most UAS, weather hazards may be extremely dangerous to their flights. Numerous UAS crashes and accidents were reported that were principally caused by hazardous weather factors. Despite of the mentioned sensitivity of UASs to weather – at present –, the number of systems that are specially developed for the meteorological support of UAS operators is relatively low (*Garcia et al.*, 2013; *Sun et al.*, 2014).

In order to decrease the weather-related risks during UAS flights, we had developed a complex meteorological support system for UAS users, mission specialists, and decision makers. This system is based on an integrated weather prediction software, the Integrated Forecasting System (IFS). Calibration and verification have been carried out using a special meteorological UAS, called the Hungarian Unmanned Meteorological Aircraft System (HUMAS). Finally, it is important to point out that this meteorological support system can easily be adopted for any location at all over the world, because the applied meteorological data and numerical model system are mainly open-access.

2. The Integrated Forecast System (IFS)

Prediction of key aviation meteorological parameters such as visibility and ceiling is one of the greatest challenges for an operational forecaster. These variables are usually the Achilles' heel of numerical weather prediction (NWP) models, too (*Jacobs* and *Maat, 2005*; *Souders* and *Showalter,* 2008; *Hirardelli* and *Glahn*, 2010). Unfortunately, most of the phenomena which are affecting flight operations are not predicted directly even by high resolution NWP models. Visibility and ceiling are playing clearly a key role in the success of UAS missions, (*Bankert* and *Hadjimichael,* 2007). Usually, the operational minima of UAS flights are below the limits of special mission execution. For example, for reconnaissance or surveillance tasks, poor visibility and low ceiling can eliminate the mission but yield no restrictions to the UAS flight itself.

Accordingly, high resolution NWP model output data should be processed parallel to a statistical analysis of archive database for a given weather situation to produce the best combination forecast in a certain occasion. To solve the challenge of visibility and ceiling prediction, we developed the Integrated Forecast System (IFS) which consists of i) a suitable, specially tuned NWP model, ii) a statistical climatological prediction component, which all together are capable to generate iii) a reliable and appropriate hybrid (combined statistical and numerical) aviation meteorological forecasts for UAS operations.

The construction of the experimental complex meteorological IFS is based on the following parts:

- statistical modeling subsystem (SMS),
- numerical modeling subsystem (NMS),
- hybrid modeling subsystem (HMS),
- post processing subsystem (PPS),
- UAS measurements (UM).

The main components of the UAS meteorological support system and the relations of its different components are shown in *Fig. 1.* The Integrated Forecast System is a modeling and post-processing unit using both statistical and numerical outputs of its subsystems to produce hybrid visibility and ceiling forecasts. IFS uses climatological data of mentioned parameters from the statistical modeling subsystem and actual weather forecast data (basic meteorological variables) from the numerical modeling subsystem. Based on these parts, IFS is able to produce the hybrid (combined) short-time predictions with respect to both visibility and ceiling. On the other hand, IFS has a coupled UAS measurement (UM) component to verify and test the IFS predictions during the development time. The applied Hungarian Unmanned Meteorological Aircraft System (HUMAS) was equipped by meteorological sensors to measure the atmosphere with special regard to the state of the planetary boundary layer (PBL).

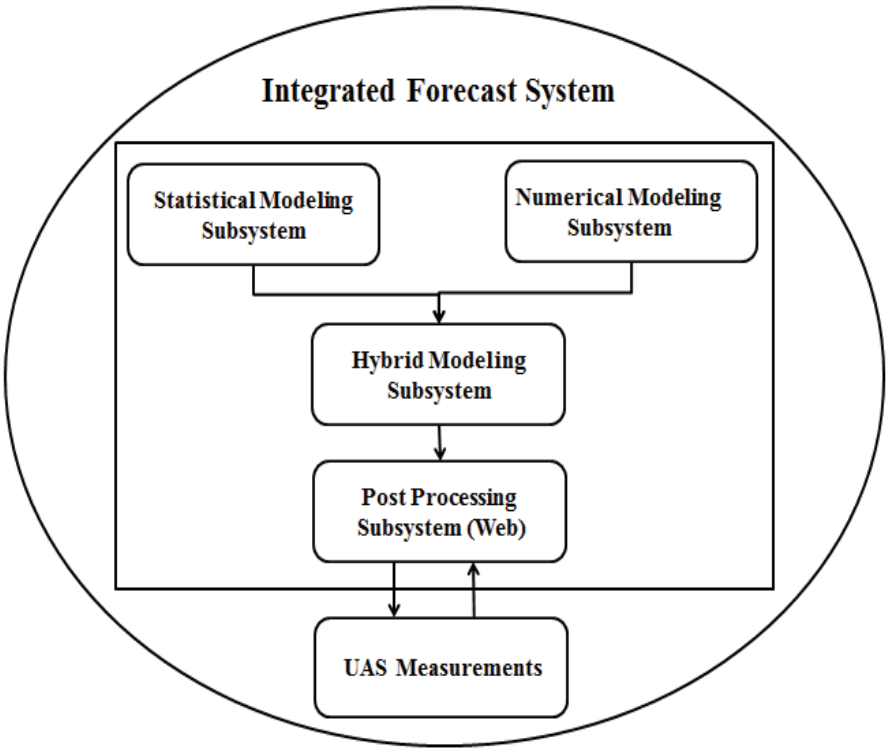

Fig. 1. The structure of the Integrated Forecast System (IFS) for UAS missions.

3. Statistical approach in the IFS

Fuzzy logic based analog forecasting is a quiet new and effective tool of ultra-short term weather forecasting (*Hansen,* 2007).

The basic principle of analog forecasting is well known (from *Toth*, 1989) as to find similar weather situations in the past to the current and recent conditions and rank them according to the degree of their similarity in the interest of giving relevant information for weather forecasts. The term *weather situation* hereafter is meant as a couple-of-hour continuous observation. Therefore, analog forecasting does not work without a relevant climatic database which contains the meteorological parameters planned to forecast in the future. We had set up an appropriate database for Hungarian military airbases (LHKE, LHPA, and LHSN) and for the largest Hungarian international airport (LHBP), based on routine aviation weather reports (METARs) (*Bottyán et al.*, 2012; *Wantuch et al.*, 2013). *Fig. 2* presents the location of airports. The applied database contains the meteorological variables for every half hour from 2006. More than 30 variables have been introduced, including the parameters both in raw and derived formats (e.g., year, month, day, hour, minute vs. day of the year). The records are more than 99% complete, and the whole database is reproducible from raw METAR reports in short time with our script (*Bottyán et al., 2012*).

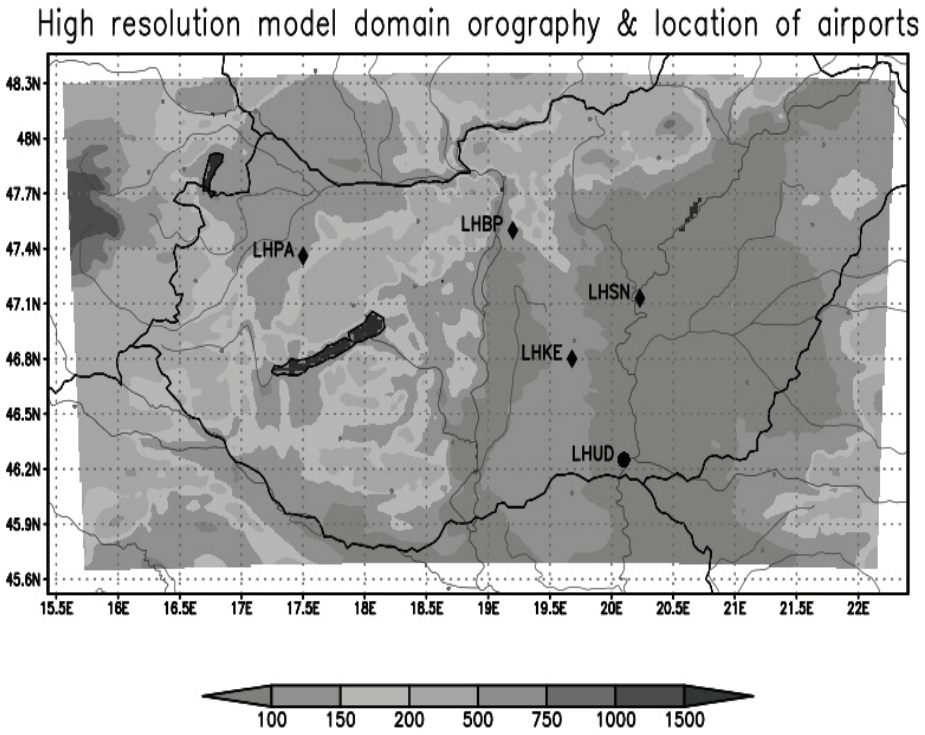

Fig. 2. Locations of four Hungarian airports inside the highest resolution, innermost (d03) model domain that were examined in the present study (black diamonds). LHKE: Kecskemét; LHSN: Szolnok; LHBP: Budapest; LHPA: Pápa. LHUD is the Szeged aerodrome (black dot), the location of field experiments.

The applied fuzzy logic based algorithm is measuring the similarity between the most recent conditions and the appropriate elements of the database. During the examination of every single weather situation, the model uses the current and the eleven previous METARs' content. The algorithm compares the meteorological variables of every examined time step using fuzzy sets *(Tuba et al.*, 2013b; *Wantuch et al.*, 2013).

The fuzzy sets – composed to describe the degree of similarity – were determined by experts (in this case by operational meteorologists), which is a common method in the development of fuzzy systems (*Meyer et al.*, 2002). These functions are applied for all compared parameters, to output the measure of similarity ranging from 0 to 1. The individual parameters at a given weather situation are examined one by one, and the overall measure of similarity for that situation is constructed from the weighted average of the individual measures of similarity of the parameters (*Tuba et al.*, 2013b).

Obviously, the initial values (or situation) of a given meteorological parameter from the most similar cases have determinative role in the forecast process. The higher the difference between initial values, the higher the risk of an inaccurate forecast of the selected element.

This led to our assumption: we could improve the accuracy of the forecast of individual elements by using appropriate weights highlighting the importance of them during the fuzzy logic based forecasting process (*Tuba et al.*, 2013b). As we have shown in our mentioned study: there are two different ways to highlight meteorological parameters which help to give more similar initial values for the parameters selected as more important. The first method is the suitable designation of fuzzy sets. Unfortunately, this approach is very difficult, because the expert judgments are hardly applicable on indirect way. In this case, they have to define the potential modification of the chosen fuzzy set in order to give a better prediction of the selected element. In another approach, we assign weights to the meteorological variables. The higher the importance of the parameter, the larger the applied weight. Because of the large number of variables, the direct determination of weights was excluded.

We applied the Analytic Hierarchy Process (AHP) introduced by *Saaty* (1977), which is a widely used technique in different fields of life except meteorology. This method is mainly used in multi-criteria decision making, especially in solving complex problems from most different fields (*Bardossy et al., 1993*; *Al-Harbi*, 2001; *Tuba et al.*, 2013a). Its main idea is to model the problem as a hierarchy. It is needed to define decision makers' goal, the applied criteria in decision making, which evaluates the possible alternatives and the alternatives to be chosen. In our case, the goal is to find the most similar situations in the database. Actually, it means the decision making. The conclusion of the lines above is that the alternatives are the single weather situations which are evaluated by the criteria: the different meteorological and time parameters. The meteorological problem to be solved has seven-seven

different criteria and sub-criteria, and more than 100,000 different alternatives. The large number of alternatives makes impossible to apply the whole analytic hierarchy process for finding the most similar situations, but for this we have the fuzzy logic based algorithm described above.

AHP was used only for determining the applicable weights for the different parameters as criteria. It was implemented by the first steps of AHP technique. Firstly, it is necessary to apply pairwise comparison on criteria which is based on general definition. In our case, these experts' judgments were assigned by operational forecasters' joint opinion. The ratios of pairwise comparisons can give the elements of a matrix. The best choice for the weight vector is the eigenvector belonging to the maximal eigenvalue of this matrix (see *Saaty*, 1977). To determine the eigenvector, we used the standard power iteration method. The received weights will be shown at the verification results. Obviously, the matrix might be inconsistent due to the subjective comparisons. We found an inconsistency of 2.5% which is less than the tolerable 10%, so the results are significantly reliable (*Saaty*, 1991).

Knowing the calculated weights we can determine the similarity of the individual time steps under investigation by weighted averaging of the single parameters' similarity. Finally, we calculate the overall similarity ($S_{overall}$) of the examined case from weighted averaging of the similarity of time steps. The current observation ($t - 0$th time step) gets the largest weight, and this weight decreases rapidly as we go through time steps. It provides that the most similar cases probably contain the dynamic changes and guarantee the convergence in similarity during the examined time period. General description of the weighted averaging is the following:

$$S_{overall} = \frac{\sum_{n=1}^{k} \left(2^{n-1} \cdot S_{t-(n-1)}\right)}{2^{k} - 1}, \qquad (1)$$

where k is the number of the time steps applied in comparisons and $S_{t-(n-1)}$ is the similarity value of the $(t-(n-1))$th time step.

After finding the most similar weather situations, we can compose a deterministic prediction from the consecutive observations of the chosen cases with an appropriate method. The model collects the 30 most similar situations which are used for producing deterministic forecast. In the semi-operational phase, we used the 30th percentile value of the chosen parameter as prediction following *Hansen* (2007). We found that the percentile value is not independent from the examined parameter and the category limit of dichotomous forecast. We plan to investigate, if the verification results could be improved by dynamically changing percentile value in the function of category limits.

4. Numerical modeling in the IFS

The Weather Research and Forecasting (WRF) model from the UCAR (*Skamarock et al.*, 2008) with the Advanced Research WRF (ARW) core, version 3.5 (release April 18, 2013) has been applied to generate numerical input for our NWP system.

WRF is a well-established, tested, and documented, non-hydrostatic, meso-scale meteorological model, applicable for both atmospheric research and weather forecasting purposes ranging from micro to global scales. Its modularity and flexibility together with its detailed documentation suited well for the needs of our purposes (*Passner et al.*, 2009). The modular structure of our development provides the possibility to swap one limited area model with another – e.g., ALADIN/AROME (*Hágel*, 2009; *Balogh et al.*, 2011; *Horányi et al.*, 2011, *Seity, et al.*, 2011) –to be used as a dynamical driver for the numerical unit of the system.

Input geographical dataset have been generated from two different sources. Landcover/land-use information were taken from the Corine 2000 (Coordinate information on the **e**nvironment) database (*Büttner et al.*, 2002) adapted and modified for the applications in WRF by *Drüszler et al.* (2011). The main advantage of this database with respect to the USGS (United States Geological Survey) dataset (originally used by WRF) is the much more realistic and detailed representation of land characteristic features (e.g., much better and more specified representation of various types of forests and scrubland; in addition to more than 3 times larger area specified as urban land). These characteristics are essential in surface-atmosphere interactions and boundary layer processes, the most valuable input for aviation meteorology parameters.

Similarly, the original FAO (Food and Agriculture Organization) soil texture dataset has also been replaced by the DKSIS (Digital Kreybig Soil Information System), produced by the Center for Agricultural Research, Hungarian Academy of Sciences (see *Pásztor et al.*, 2010 for more details). The false over-representation of clay and loam type soils within the FAO data has been removed from the input data, and sand (absent from the original database) and sandy clay have been introduced in an additional extent covering more than 12% of the area of the country. The spatial distribution of the difference between the two different input data with respect to landuse (USGS vs. Corine 2000) and soil texture (FAO vs. DKSIS) geographical data fields are depicted in *Fig 3*. The most significant differences are the representation of urban area, water bodies and the under representation of evergreen forests in mountainous area, while with respect to soil texture. Contrarily to the Corine 2000 database, which covers whole Europe and can be applied to all model domains, DKSIS covers only the area of Hungary, inside the political boundaries of the country and is usable only for the best resolution (d03) domain (*Fig. 4*).

In addition, soil hydraulic parameters used by the WRF model were modified according to Hungarian soil sample data (MARTHA and HUNSODA), giving more realistic values for the soil structure in Central Europe (*Ács et al.*, 2010). Sensitivity tests showed that even during a sunny summer day, model results featured significant differences in terms of planetary boundary layer heights with respect to the soil hydraulic parameters that have been applied (*Breuer et al.*, 2012; *Ács, et al.*, 2014).

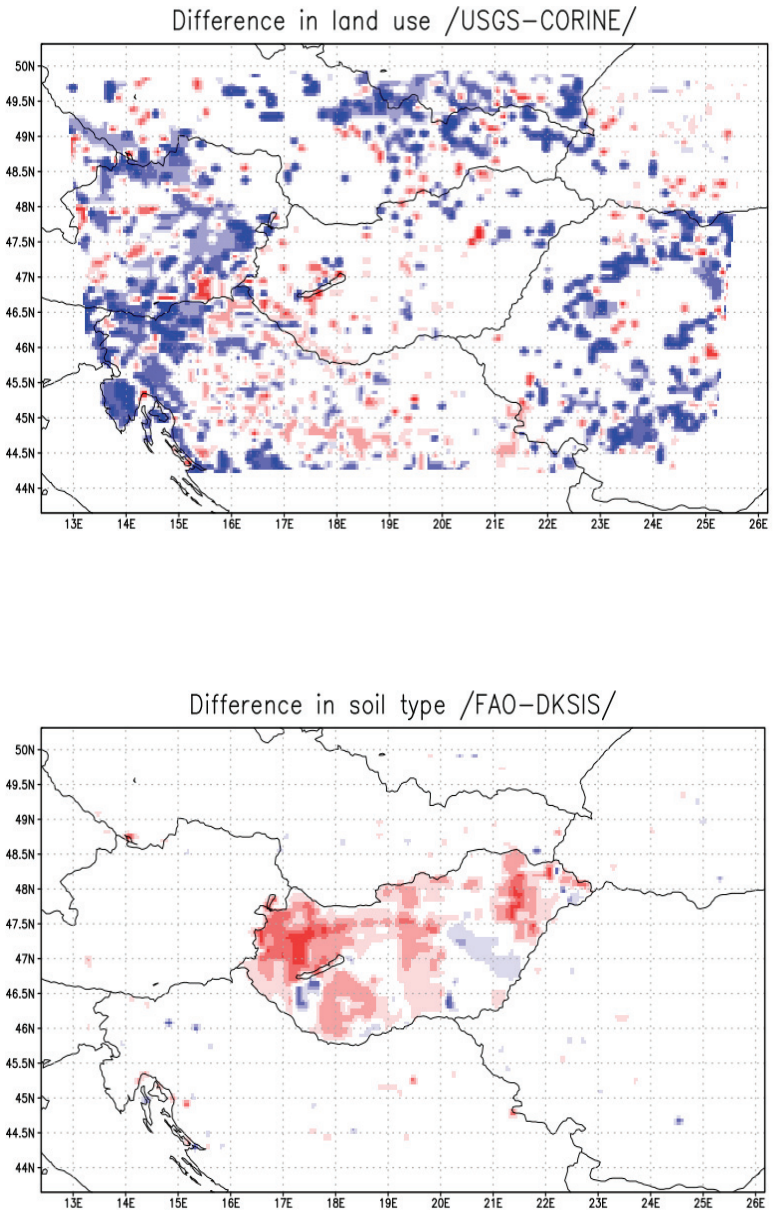

Fig. 3. Differences between the original and replaced geographical data with respect to land use (top) and soil texture (down) databases, applied for the integration of the WRF numerical weather model. Red (blue) shades indicate areas where the land use index has been increased (decreased), and white areas were not changed. It can be seen, that for soil texture, only the area inside the political boundaries of Hungary was modified.

The model setup in the newly developed IFS is the following. The number of vertical levels is 44, from which 24 levels are below 2 km. The vertical layers depth is ranging from 25–250m in the lower portion of the domain through 500 m layer in the middle levels up to 780 m in the upper portion of the model domain (see *Fig. 4*, left panel). Three level telescopic nesting is applied ranging from 22.5 km in the coarsest (d01) domain through 7.5 km in the intermediate (d02) domain to 2.5 km horizontal resolution in the high resolution lowest (d03) nested domain that is located in the Carpathian Basin (centered N47.43; E019.18) and covers Hungary with 202×121 grid cells (*Fig. 3.*, see also *Gyöngyösi et al.*, 2013 and *Fig. 4*, right panel).

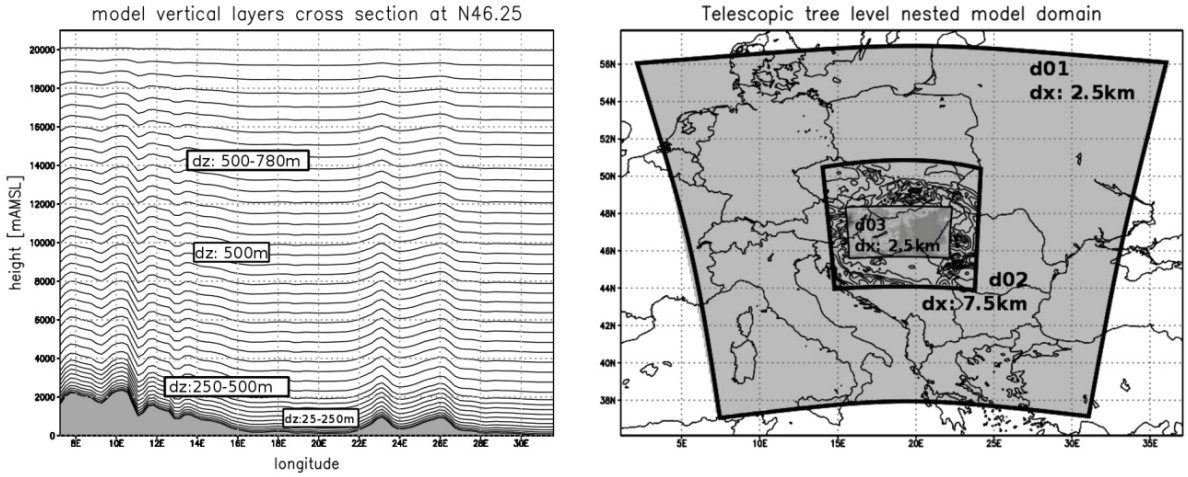

Fig. 4. Vertical levels with higher resolution in the lower levels and deeper layers in the upper portion (right panel) and the three level telescopic nested domain setup for high resolution modeling of the Carpathian Basin in the IFS system (left panel). Horizontal resolution is 22.5 km, 7.5 km and 2.5 km, grid size is 97×97, 97×97, and 202×121, respectively.

In order to apply a setup tuned for the special requirements of the designated purpose, extensive tests were performed: 30 different combination of parameterization setups (*Gyöngyösi et al.*, 2013) – including 8 types of micro-physics (types 3–9 and 13), 6 types of land surface models (types 1, 2, 4, 5, 7 and 10), and 8 types of PBL (1, 2, 4, 5, 7–10) schemes (see WRF-ARW Version 3 user's manual, *Wang et al.*, 2009) – have been tested. Tests have been performed for 9 selected weather situations, all having aviation weather relevancies (*Table 1*). Similar investigation has been made by *Hu et al*. (2010) for the optimization of the modeling of PBL processes with the comparison of three different parameterization schemes. An extensive test with a physical ensemble, using different parameterization setup (e.g., *Evans et al.*, 2012) requires enormous computational capacity, while in the current project we were focusing only to the study of a limited number of typical weather situations.

The test case studies investigated in the current test were chosen according to their aviation meteorology relevance, all of them are typical in the Carpathian Basin, including heavy icing, deep convection, abrupt wind direction change, etc. The list of the cases is detailed in *Table 1.*

Table 1. Test cases (date and short description) of weather situations for the evaluation of the numerical weather prediction unit

No.	Date	Description
1.	10.27.2012.	Widespread precipitation from a Mediterranean low pressure system
2.	09.20.2012.	High horizontal pressure gradient situation with strong winds, with a special wind pattern
3.	01.19.2012.	Significant low-level inversion during winter period
4.	09.08.2012.	High pressure ridge transition resulting in significant and rapid change in wind direction
5.	07.29.2012.	Deep convection resulting in local and heavy showers that were not well resolved by most operational models
6.	05.12.2012.	Significant change in wind direction following a cold front
7.	01.22.2012.	Well documented severe icing case weather situation
8.	02.16.2012.	Convective precipitation from a high level cold vortex, temperature in the mid-troposphere is less than –25 ^{o}C
9.	12.06.2012.	UAS test flight case for direct verification purpose

Model output have been compared to synoptic surface observations at 31 ground stations in Hungary located in the high resolution (d03) domain, and operational radiosonde data of 4 stations located in the medium resolution (d02) domain. Temperature, dew point, and wind data have been compared using RMS error and a wind score derived with respect to wind speed and wind direction differences. Results showed that in the surface data there is a wide variation in humidity and temperature, while in the upper level only wind speed and direction are significantly affected by the choice of the parameterization schemes.
From the analysis of the results the Bretherton and Park (2009) moist turbulence PBL scheme, the WRF Single Moment Scheme with 3 micro-physics class

(*Hong et al.*, 2004) and the Noah scheme (joint development of the National Centers for Environmental Prediction, Oregon State University, Air Force and Hydrologic Research Lab) for land-surface processes (*Chen* and *Dudhia*, 2001) performed the best. For parameterization the RRTM (Rapid Radiative Transfer Model) for longwave radiation (*Mlawer et al.*, 1997), the *Dudhia*'s (1989) scheme for shortwave radiation and a modified version of the Kain-Fritsch scheme (*Kain*, 2004) for cumulus convection parameterization have been applied.

GFS data with $0.5^{\circ} \times 0.5^{\circ}$ resolution was applied as initial and boundary conditions for the limited area integration of the outermost domain in every 3 hours, with no additional data assimilation. Soil temperature and humidity data were taken from GFS model as initial data only and were handled separately from meteorological data as boundary conditions, i.e., it is not updated from the large scale model during the integration. Appropriate adjustment of the lower boundary conditions to the physics of the model was achieved during the spin-up period in the beginning of the model integration. Input data was prepared with WPS, the vendor preprocessor of the WRF system.

This model setup has been considered as the best choice for the current purpose and it has been kept for operational integrations that are being run for 96 hours lead time, performed two times a day, initialized from 00 and 12:00 UTC, and 04:00 and 16:00 UTC, respectively. Data download of 1.5 GB input data from NOAA server takes 40 minutes, model preprocessing and integration on 24 cores for about half an hour, and post-processing for another 40 minutes. Model products are delivered to the users through the web interface of the integration server itself 6 hours after initialization time.

For the need of UAS forecasts, two different post-processors (ARWpost and the Universal Post-processor, UPP) are used. Output data is interpolated to both pressure levels (with UPP) and height levels (with ARWpost). Times series of predicted values at selected locations for (QNH) pressure; wind speed, direction (barbs), and wind gust; temperature, dew point, trigger temperatures for 1000 m and 1500 m deep thermal convection; grid scale and convective precipitation (both accumulated and intensity); and different level cloud amount, low-level cloud base (ceiling), and visibility forecasts are also published operatively (*Fig. 5a*).

In order to support UAS operation in the lower troposphere (from surface up to 3000 mAMSL) and above (up to 7000 mAMSL), evolution of vertical profiles (time-altitude cross-sections) of wind, temperature, lapse rate, and humidity are also plotted using shading and contouring at certain height levels (instead of pressure levels), that are easily interpretable by the user (*Fig. 5b*). Model prediction is presented in the usual form for the days of the intensive PBL observation period at Szeged, from in November 27–30, 2013 (*Cuxart et al.*, 2014; *Weidinger et al.*, 2014).

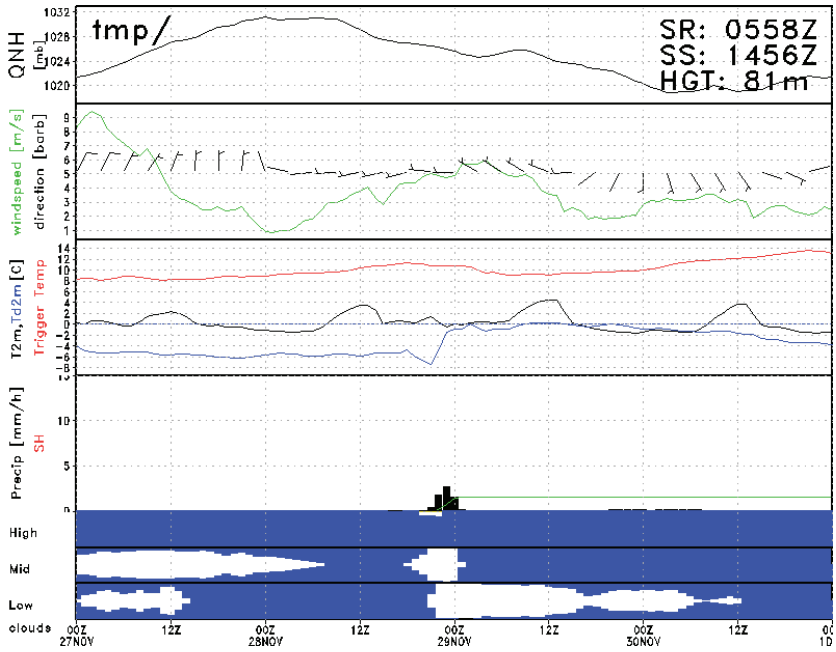

Fig. 5a. Meteogram graphical output of the predicted time variation of surface meteorological variables. Description of variables depicted on each panel, from top to bottom: sea level pressure (QNH), wind speed (green line, m s^{-1}) and direction (barbs), 2 m temperature (black line), dew point (blue line), and the calculated trigger temperature for a 1500 m mixed convective layer (red line), precipitation intensity (black bars), accumulated precipitation (green line), and low-, medium-, and high level cloud amount (white shaded area in the respective blue strips) with respect to time (UTC, horizontal axis), in the form as delivered to the users through the web based interface. Calculated sunrise and sunset times (UTC) are printed on the top right corner together with surface elevation.

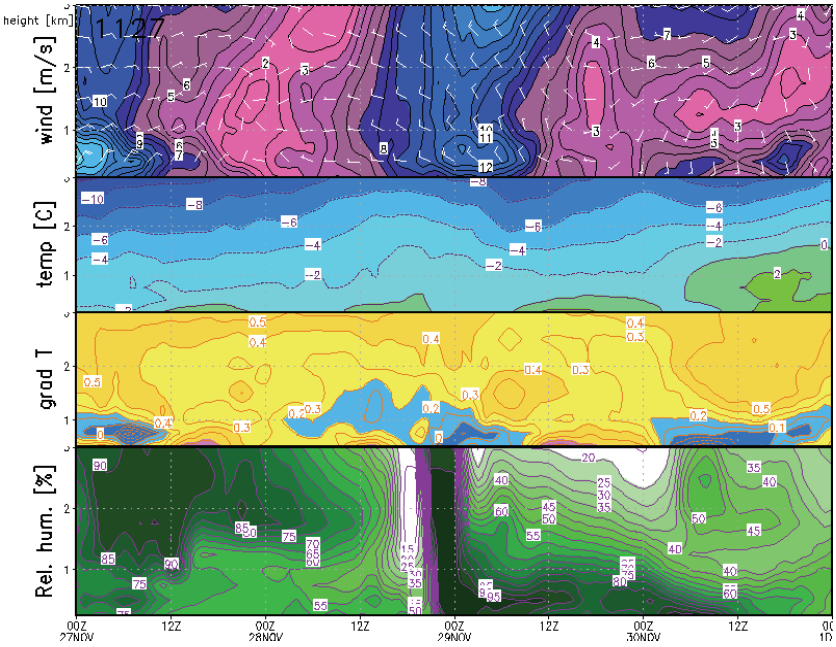

Fig. 5b. Same as *Fig 5a.* but for vertical profiles of atmospheric variables: wind speed and direction (barb), temperature, vertical temperature gradient (lapse rate, blue shades for absolute stable, yellow shades for conditionally unstable, and red shades for unstable stratification), and relative humidity.

In addition to basic model forecasts, time series of derived aeronautical weather parameters are also given (*Gyöngyösi et al.*, 2013). For example, predicted thermal characteristics (temperature advection, condensation level convective layer height, thermal index profile, and expected convective vertical velocity) can also be seen on a separate page for all locations. Visibility is computed using both the built-in scheme of UPP and the decision-tree based algorithm developed by *Wantuch* (2001), including FogSSI as a function of predicted temperature at the surface and 850 hPa level dew points (T_d) and the wind speed at 850 hPa.

Derived icing and turbulence forecasts are plotted on time-vertical cross-sections using different methods for the estimation of the intensity of processes (*Mireles et al.*, 2003; *Sousounis*, 2005; *Fövényi*, 2010).

5. Hybrid visibility forecasting in the IFS

Applicability of statistical (i.e., analogy based) and numerical forecasting of visibility is limited. Analog forecasting is based on a special database and on the measured information of the actual ($t + 0$) weather and a short period before. Its efficiency (accuracy or reliability) decreases over time. On the other hand, the performance of NWP model is basically constant over the examined short forecasting period (nine hours time interval). The correlation coefficients between category differences – which are based on the difference of numerically predicted and observed visibilities (*Bottyan et al.*, 2013; *Wantuch et al.*, 2013) – at the initial ($t + 0$) and latter time steps show also gradual and significant decrease over time (*Fig. 6*). Five visibility categories are used within the 0 – 800 m, 800 – 1500 m, 1500 – 3000 m, 3000 – 5000 m, and above 5000 m intervals initially, the possible absolute category differences are 0, ±1, ±2, ±3, and ±4, respectively.

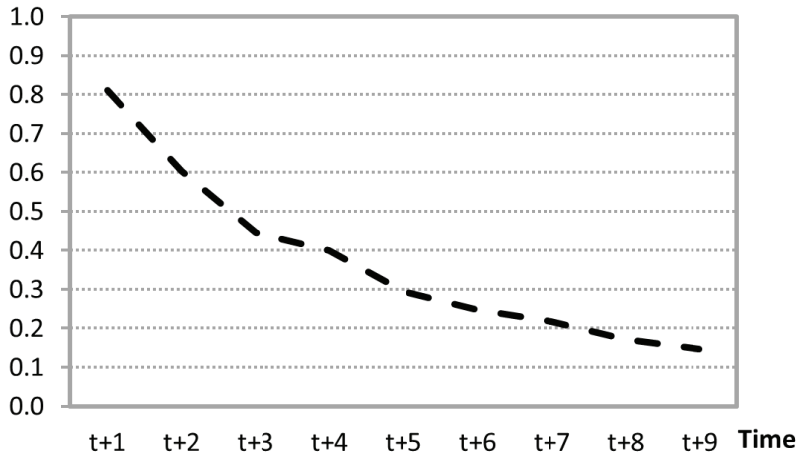

Fig. 6. Correlation coefficients of category differences between numerically predicted and observed visibility at the initial ($t + 0$) and latter time steps.

Preliminary results showed that the error of the initial time step is in close correlation with the latter inaccuracy of forecast from the same model run, but only for an ultra-short time period. This gave us the idea to combine the different methods during this period keeping their advantages and eliminating their disadvantages at the same time. This kind of models run only every 6 to 24 hours, thus the incorrect forecasts can be amended after the next model run which means the same loss of time. In contrast, the refresh rate of statistical forecasts fits the observation frequency which is not more than 1 hour. In consideration of the above, we created this hybrid model, which is from the simple linear combination of the statistical and numerical model outputs (*Tuba, 2014*):

$$Visibility_{HYBRID} = a \cdot Visibility_{STAT} + b \cdot Visibility_{NUM} \quad , \tag{2}$$

where $a + b = 1$ and $a, b \in [0; 1]$. We specified that the statistical prediction weights should decrease

- with increasing category difference, because it corrects the potential initial inaccuracy of numerical model, and
- monotonically over time to provide the gradual transition between the statistical and numerical methods (*Bottyan et al.*, 2013).

On the basis of the above mentioned things, we can compose a weight matrix, with rows for the absolute category differences and columns for the time steps. *Table 2* gives an example for this kind of matrix with statistical model weights. Weights are optimized by verification parameters as absolute and root mean square error.

Table 2. The potential weights of statistical model are based on an experimental experts' first guess was examined on the LHSN data in the August 2013 and February 2014 period

		t+1	**t+2**	**t+3**	**t+4**	**t+5**	**t+6**	**t+7**	**t+8**	**t+9**
Absolute category difference	**4**	1.00	1.00	1.00	0.90	0.80	0.65	0.50	0.35	0.20
	3	1.00	1.00	0.90	0.80	0.70	0.55	0.45	0.30	0.20
	2	1.00	0.90	0.85	0.75	0.65	0.50	0.40	0.25	0.15
	1	0.90	0.85	0.80	0.70	0.60	0.45	0.35	0.20	0.10
	0	0.90	0.80	0.70	0.60	0.50	0.40	0.30	0.20	0.10

6. The Hungarian Unmanned Meteorological Aircraft System (HUMAS)

In the Hungarian Unmanned Meteorological Aircraft System (*Mikó et al.*, 2009; *Szabó et al.*, 2013) for meteorological UAS measurements the BHE Bonn UAS has been mounted with the meteorological system as described below. The main features of the aircraft are the following: 16 kg total weight with 3 kg maximum payload, electrical propulsion that provides around 60–90 km/h IAS cruising speed, approximately 60–90 minutes duration, and more than 3000 mAGL flight altitude. The aircraft is equipped with a two-way microwave data communication system with a range of 15–20 km. The meteorological system is autonomous, independent of the UAS flight system, with its own power, GPS, IMU, and other sensors. It can be easily mounted on any other platform such as multi-copters or balloons.

The meteorological system is composed of a central unit and sensor units. The central unit (CU) is responsible for collection of the sensor unit (SU) data, pre-processing, and logging as well. The CU contains the power supply for the system, the onboard computer, and an UAS key for the data storage as shown below (*Table 3*).

Table 3. The structure of the central unit (CU)

Device	**Application**
BeagleBone A6 single-board-computer	Pre-processing and logging. Features: 700MHz ARM Cortes-A8, Linux OS on micro SD card, 256MB DDR2
Replaceable USB-key storage	Collecting of SU data
Power supply	Power supply for the independent meteorological measurement system. 7.4V, 3300mAh Li-Po with 2 cells providing > 6 hours duration depending on SU setup

The SU contains all those instruments that necessary for collecting data usually provided by radiosondes. Because of the fast climbing and sinking rate during airborne measurements, it is necessary to sampling in a high frequency, particularly in temperature and relative humidity measurements (*Martin et al.*, 2011). According to this expectation, two sensors were placed on the HUMAS: a Vaisala HMP 45 (slow sampling) and a Texas Instruments TMP102 with a high frequency sampling rate (*Table 4.*). The sensors were mounted on the top part of the HUMAS's nose in a well perfused box (*Fig. 7*). The Vaisala probe was shielded with a white PVC tube with holes. The high sampling rate gave us an opportunity to measure not only vertical profile but temperature and relative humidity anomalies in up- and downdrafts during horizontal flight path (*Reuder et al.,* 2009).

Table 4. The structure of the sensor Unit (SU)

Device	**Measured variables**	**Derived variables**	**Sampling frequency (Hz)**	**Accuracy**	**Resolution**
TMP102	Temperature		10	0.5°C	0.0625°C
HIH-4030	Relative humidity		10	±3.5%	0.5%
BMP085	Pressure	Barometric altitude	10	±1.0hPa	±0.2hPa
GPS uBlox 6 SPK-GPS-GS407A 50 Channel	φ, λ	Ground speed, Track	4		Horiz. <2.5m
3-Axis MEMS accelerometer, 9-Axis MotionFusion	Euler angles (Θ, φ, ψ)		100	16384 LSB/g	±16384 LSB/g
HMC5883L 3-Axis digital compass with Atmega328 microcontroller	Magnetic direction (MagX, MagY, MagZ)	Heading	100	1370LBS /gauss	1°
Vaisala HMP50	T		1	±4.0%	1%
Vaisala HMP50	RH		1	±0.6°C	0.1°C
Prandtl-tube with HCLA 12X5EU and HCA-BARO pressure sensor	Pdin, Pstat	IAS, Barometric altitude	100	±6Pa, ±5mbar (baro.)	
5HP with HCLA 02X5EB and HCLA 12X5EU pressure sensor	Pdin, Pstat	IAS, Barometric altitude, Angles of attack: α, β	100	±2.5Pa	

The system included GPS, accelerometer, digital compass, and the Prandtl-tube or the 5HP five holes probe that allowed us to apply several wind estimation methods, however, new methods were developed for wind measurements which have a lower instrumentation demand (*Szabó et al. 2013*). With the five holes probe (5HP) developed by the Technical University of Budapest (*Varga* and *Balczó*, 2013), high frequency 3D flow data became available (*Fig. 7*). With the combination of the measured 3D flow field and the temperature and humidity data, sensible and latent heat flow, could be investigated (*Bonin et al., 2013*).

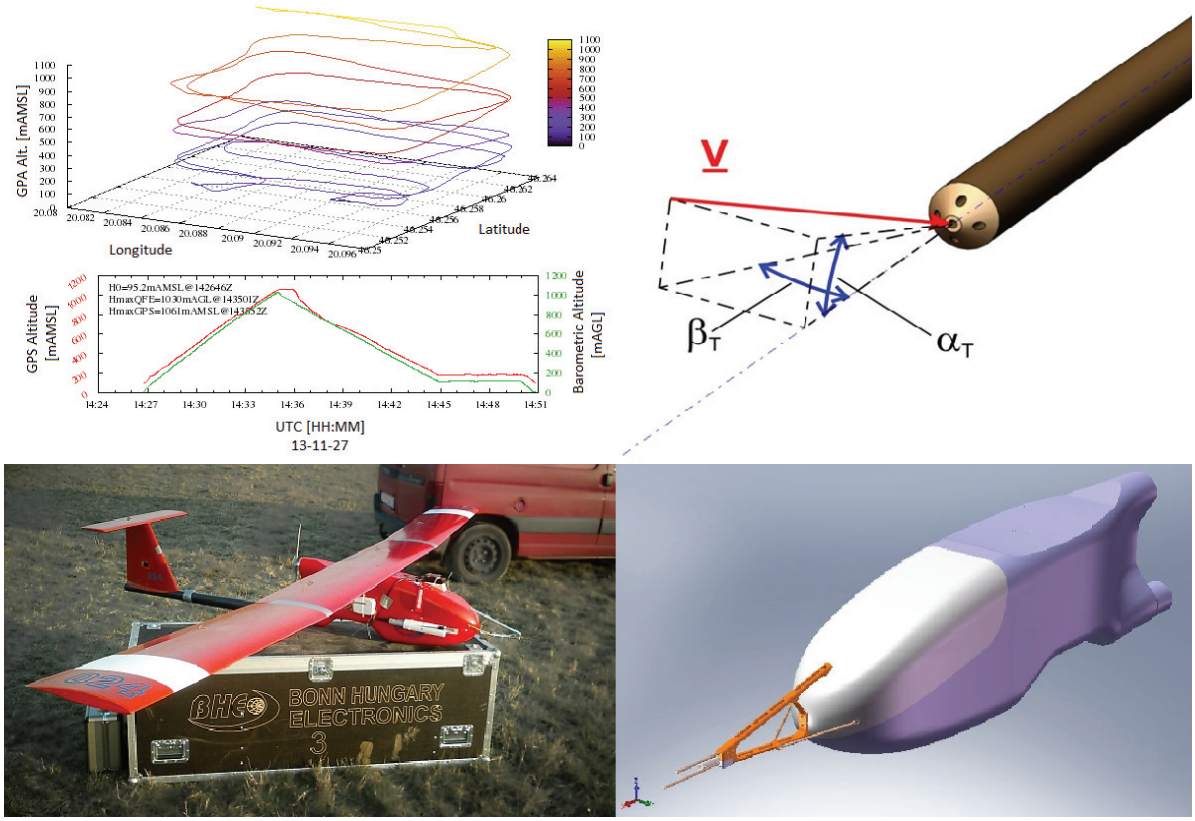

Fig. 7. Track of flight No. 4, Szeged, November 28, 2013 during the PABLS-2013 international measurement campaign (upper left), picture of the HUMAS (bottom left) and the 5HP pressure sensor (upper right) and its mounting on the nose of the HUMAS (bottom right).

7. Preliminary results and discussion

After the description of the statistical, dynamical, and hybrid forecast system, followed by the presentation of the UAS based meteorological aircraft system, hereafter the applicability of the development will be demonstrated. In the following section the evaluation of the visibility forecast of a longer period of case is followed by the presentation of the preliminary results of an international atmospheric boundary layer observation campaign, where the system has been tested and performed suitable.

7.1. Visibility forecast

In order to show the efficiencies of developed analog visibility forecasting model, the whole climatic database was divided into two different and

independent parts. The first one is for searching analog weather situations using fuzzy logic to the selected reports which are from the second dataset and they represent its every third hour. This control dataset contains the available and selected weather information of 2012. Nine-hour-long categorical forecast was examined (*Bottyán et al.*, 2013). The number and interval of categories are easily changeable in the verification template, so we can control the dependency of the results due to the different values.

Doswell et al. (1990) showed that there is no omnipotent verification method. For comprehensive verification of forecasts, it is advised to use several skill scores and verification parameters (*α*, *BIAS*, *POD*, *POFD*, *FAR*, *HIT*, *CSI*, *TSS*, *HSS*, etc – see *Nurmi*, 2003). To the calculations we used a 2×2 contingency table of different categories of the parameter under verification (*Table 5*). As described in *Bankert* and *Hadjimichael* (2007): "Heidke skill score (*HSS*) is computed to measure the performance of each algorithm relative to random chance". Positive, zero, or negative *HSS* value indicates better, no better, or worse forecast performance than random chance, respectively. It is very important to note, that HSS values remain correct with verification of rare events, which is typical in case of low visibilities. According to the reasons, we present mainly the *HSS* values of visibility forecasts of the different prediction methods.

Table 5. Contingency table for categorical forecasts of binary events

		Event observed	
		YES	**NO**
Event forecasted	**YES**	**a** (hit)	**b** (false alarm)
	NO	**c** (missed)	**d** (correct rejection)

Some naive forecasts (e.g., persistence) can be a standard of reference *Murphy* (1992), or in other words, a competitive benchmark in the field of short term forecast verification. Thus, we show the verification results of persistence forecast on every figure for the comparability of outcomes. As it can be shown in *Fig. 8,* analog statistical forecast was generated for every third hour of the control period applying two different methods. Firstly, we did not use weights for highlighting the importance of the forecast element; secondly, we applied the calculated AHP weights. Each of them means almost 3000 model runs per examined airports (LHSN, LHPA, LHKE, and LHBP) in 2012.

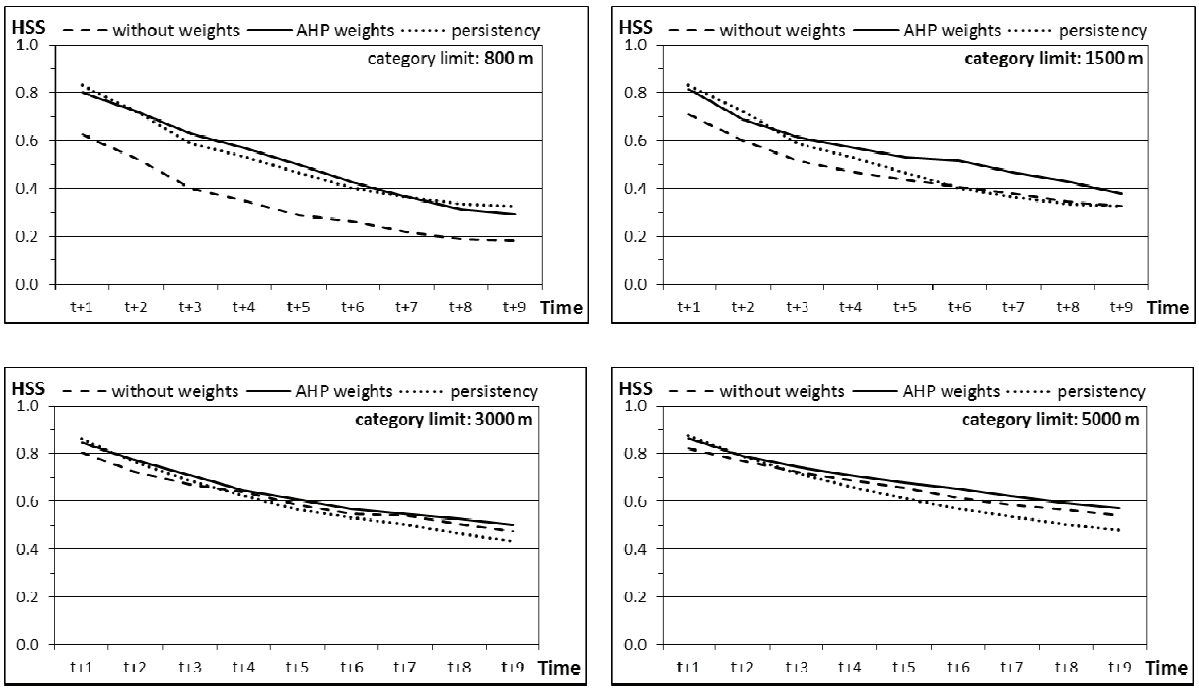

Fig 8. Average *HSS* of examined Hungarian airports (see *Fig. 2*) for predictions of different category limits and for the applied forecast methods for the year of 2012.

Then we calculated the *HSS* values for both the methods and all of the examined category limits (800 m, 1500 m, 3000 m, and 5000 m), as well as the persistence forecast.

We found that application of AHP weights improved significantly the performance of analog forecasting during the whole nine-hour forecasting period. It is especially true in case of lower visibility ($\leq$ 1500 m). The applied AHP weights make analog forecasting highly competitive with persistence forecast in these categories.

In the following we show a case study, which represents how the hybrid model can correct the different visibility forecasts. On December 23, 2013, the synoptic situation over Central Europe was determined by anticyclonic effects. In Hungary, the weather was misty and foggy in several places day long. Only weak cold front touched the northern part of the country, and it caused some changes later. In Szolnok Airport (LHSN, 12860) there was broken or overcast ceiling at 4000 m during the previous night. Due to the clouds, the visibility decreased only to 3000 m. The clouds did not help the improvement of visibility during daytime. In the early evening hours the clouds became scattered, and due to the radiation, the visibility started to decrease rapidly, and finally dense fog formed by 21 UTC.

The most important part of this situation for us is the forecast period which starts at 15 UTC. The nine-hour time period covered the formation of fog. The

numerical forecasts were from the 12 UTC model run, and the statistical model used data from the 14:45 UTC and the previous observations. This case study intentionally uses the situation described aboave, when the numerical forecast is significantly different from the observation at the initial time step ($t + 0$). *Fig. 9* shows the observed and forecasted visibility values calculated by the different models.

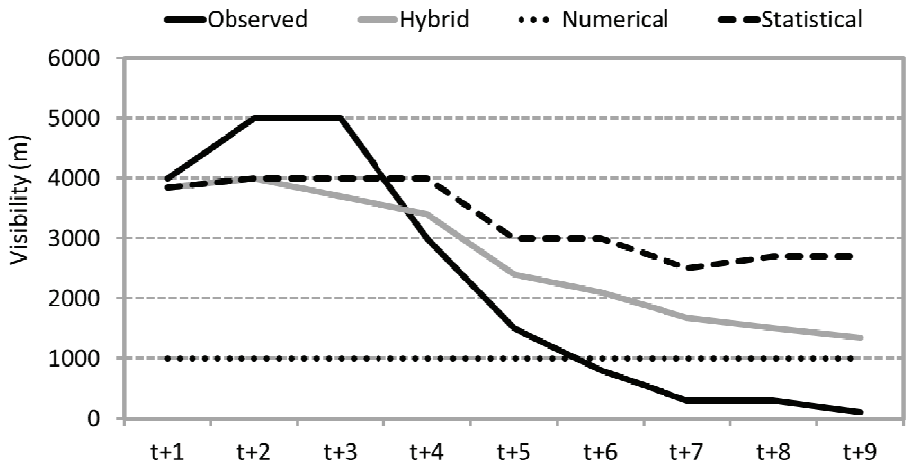

Fig. 9. The observed and different predicted visibility values for Szolnok Airport (LHSN, 12860) on December 23, 2013 ($t + 0$ = 15 UTC).

The lowest output value of the out-processing method of the numerical forecast is 1000 m. It means in the practice, that fog formed at the location. In the first part of the forecasting period, the numerical model significantly missed to correctly predict the visibility. In the second part, the statistical model missed to forecast the decreasing amount of clouds, and due to this, its visibility forecast was incorrect after that. In this situation, the hybrid model provides the best performance in forecasting visibility.

7.2. PBL profiles from HUMAS measurements and model forecasts

In the following part of this section, the preliminary results of an international measurement campaign in late November, 2013 at Szeged, Hungary is discussed, on which the HUMAS has been deployed and performed suitable.

In the first iIntensive operation periods (IOP), on November 27 and 28, 2013, during the Pannonian Atmospheric Boundary Layer Experiment (PABLS-2013, in November 25–30, 2013), Szeged was located between a high pressure system over Central Europe and a low one over the Balkans. Airflow was from E-

NE to W-SW, and layer clouds between 800 m and 3000 m could be observed. Not far from the site, to the North of latitude N45.5°, the sky cleared up and remained clear during the whole night, but stayed overcast with occasional snow falls over Szeged. After 2300Z, precipitation stopped and cloud cover decreased from OVC to BKN, and finally to FEW clearing up until sunrise (0558Z). Altogether five different HUMAS measurement flights were performed before sunset and after sunrise. The main characteristics of the flights are summarized in *Table 6.* In this section, the WRF model results of the high resolution (d03) domain will be compared to UAS measurements, and also to other data from different sources with respect to temperature, humidity, and wind features.

Table 6. Main characteristics of the HUMAS flights during the PABLS-2013 measurement IOP1 on November 27–28, 2013. T/O time is the take-off time in UTC, Flt time is the flight time seconds, Hmax is the maximum height above ground level, achieved during the flight, T range, Rh range, and p range: temperature, relative humidity, and pressure maxima and minima, respectively

No.	T/O time [day UTC]	Flt time [sec]	Hmax [m]	T range [°C]	Rh range [%]	p range [hPa]
1	27. 10 29:19	847	530	–3.4/2.5	66.8/88.1	955/1014
2	27. 12 49:37	674	483	–2.4/2.9	66.4/81.9	961/1015
3	27. 14 26:46	1444	1030	–5.9/5.9	62.4/93.9	901/1016
4	28. 06 04:28	2813	1979	–6.3/-0.2	63.3/91.9	806/1020
5	28. 09 34:41	3166	2178	–5.9/0.2	48.1/84.6	800/1021

Flight patterns have been selected to ensure maximum measurement accuracy with respect to meteorological variables, especially the calculation of wind components from GPS ground speed, (Prandtl-tube) IAS (indicated airspeed), and magnetic data. The flight path followed vertically staggered, quadratic path, keeping altitude for 3 legs and ascending/descending to the next level on the 4th leg, respectively (*Fig. 7*). Wind component speeds have been calculated from the ground speed differences on counter direction legs, and corrected with airspeed and magnetic data (*Cho et al.*, 2011; *Szabó*, 2014). In addition to onboard thermometers and humidity sensors, the UAS carried an additional Vaisala RS92-SGP radiosonde measuring unit for calibration purpose. During the IOP, the vertical flow structure of the site has been monitored with a SODAR equipment (METEK PCS.2000–24) in the lower 400 to 500 m layer.

From the comparisons, only for flight No. 4 will be presented here (*Figs. 10–11*). This flight has been carried out during the morning transition on the dawn after the night of 28 of November 2013.

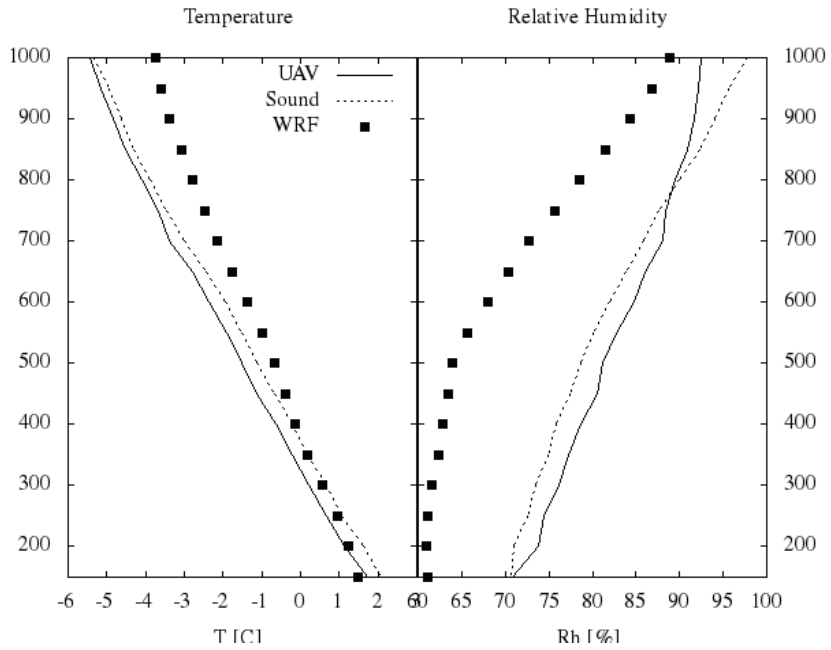

*Fig. 10.*Temperature and relative humidity data comparison. Measured data (HUMAS – solid line) is compared to measurements by operational Vaisala radiosonde device onboard of HUMAS (dotted line) and to the predicted data of the numerical weather model (high resolution, (d03) nested WRF domain – black squares). Flight No. 4, Szeged, November 28, 2013.

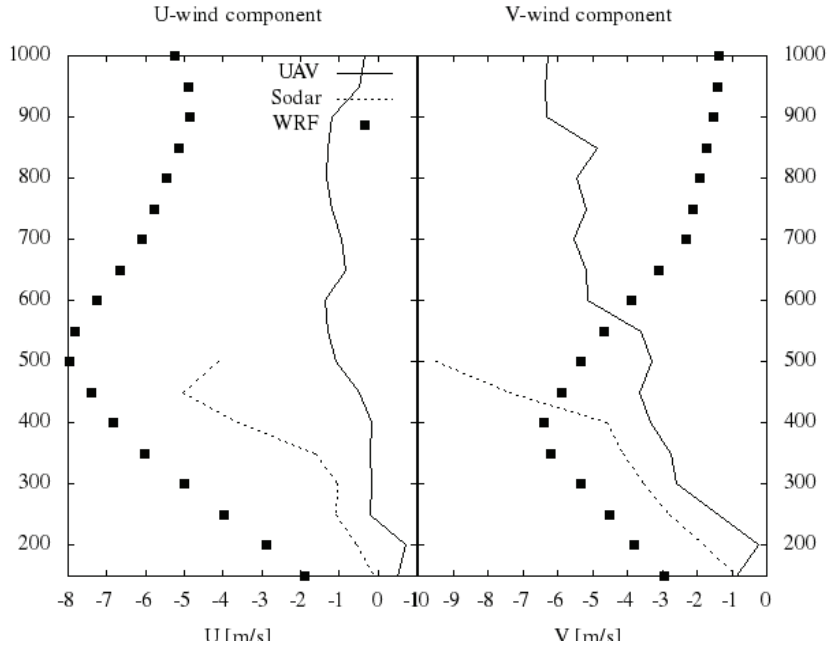

Fig. 11. Wind speed components *U* (zonal) and *V* (meridional) data comparison. Measured data (solid line) is compared to measurements by METEK PCS.2000-24 SODAR (dotted line) and to the predicted data of the numerical weather model (high resolution, (d03) WRF nested domain – black squares). Flight No. 4, Szeged, November 28, 2013.

In order to verify the measurements to standard meteorological sensors, temperature and relative humidity data were compared to a normal Vaisala RS92-SGP radiosonde unit that was carried onboard. From the qualitative comparison of *Fig. 10* it can be seen, that the temperature measurements were a little bit underestimated (negative bias), while humidity data provided by the HUMAS were a little higher than the reference, yielding an overestimation in the measurements. Comparing the measurements to modeled data shows that the model predicted more stability in the lower layer than the real temperature lapse rate, that might be a result of the under prediction of layer clouds and humidity (and of radiative cooling near surface) compared to realistic conditions in the lower layers. This sort of under-prediction in terms of humidity is clearly visible on the right panel as well, where the modeled relative humidity curve differs significantly from both measurements, especially in the lower 800 m layer. In *Fig. 11* data are presented in a manner same as in *Fig. 10* but for *U* and *V* wind components. Here the measured data has been compared to SODAR detection in the lower 500 m layer.

From the comparison of SODAR data to HUMAS measured wind data it can be seen, that there is a significant difference between the data over 300 m AGL. It should be noted however, that other wind measurements during this campaign yielded much better agreement to SODAR data than in this case, and the SODAR measurements over 300 m in certain meteorological conditions are slightly unreliable. Provided that the SODAR data are unreliable in this case over 300 m and if we consider the wind measurements of HUMAS as accurate, we can verify our model results to UAS measurement. It should be pointed out that the model predicted wind direction relatively precisely, but performed poorly in terms of wind speed, yielding in significant overestimation for wind speeds.

According to the preliminary results above, it should be pointed out that HUMAS proved to be a suitable platform for micro-meteorological in-situ measurement of the atmospheric boundary layer. Its operational costs and flexibility are much more suitable to the possibilities and needs of PBL measurements. As pointed out by *Passner et al.* (2009), *Marius et al.* (2012), *Stenmark et al.* (2014), for example, UAS measurements can yield valuable atmospheric data not only for experimental research but it may become an operational source of data for regional model calculations in the near future.

8. Conclusions

Proper, detailed, and significant meteorological support is essential during the planning and executing phases of civilian and military UAS missions. For the smooth operation of such systems, it is very important to generate accurate, high-resolution, short-time predictions of ceiling, visibility, turbulence, icing, and other aviation meteorological factors.

The meteorological support system for UAS missions described in the current paper is based on the followings parts:

- an adequate data base of four Hungarian airports derived from freely accessible METAR data,
- application of statistical, dynamical, and special hybrid methods that can help the forecaster to give prognostic information for the UAS pilots and specialists,
- specially tuned and set-up numerical weather prediction model which can provide high resolution weather prediction over the Carpathian-basin,
- special post-processing system which is based on model products for the prediction of some hazardous weather phenomena such as low visibility and ceiling, turbulence, wind shear, icing etc.,
- a special web site to deliver adequate meteorological information in graphical, text and other formats via (mobile) web connection, and
- the first Hungarian meteorological UAS (HUMAS) specially equipped for the purpose of boundary layer measurements, which has been developed and successfully used during the mentioned project.

In the future, we can give the flight path optimization based on our predicted weather situation, and also we continue the development and testing of our UAS-based airborne meteorological measurement system.

Acknowledgement: The authors thank *Károly Kazi* for using of Bonn Hungary Ltd's UAS system and *Péter Szalóky* for the AIRMET data set. Great thanks for providing the dataset during Pannonian Atmospheric Boundary Layer Experiment Szeged (PABLS-2013) to *Joan Cuxart Rodamilans*, *Gemma Simó Diego*, *Burkhard Wrenger*, *Dávid Tátrai, István Aszalos, Szabolcs Rózsa, Árpád Bordás, János Unger, János Józsa,* and *Melinda Kiss*. This research supported by the European Social Fund (TÁMOP-4.2.1.B-11/2/KMR-2011-0001 and TÁMOP-4.2.2.C-11/1/KONV-2012-0010 projects). Financial support by the Hungarian Scientific Research Foundation (OTKA, project no. K83909 and no. NN109679) is also gratefully acknowledged.

References

Ács, F., Horváth, Á., Breuer, H., and *Rubel, F.*, 2010: Effect of soil hydraulic parameters on the local convective precipitation. *Meteorol. Z. 19,* 143–153.

Ács, F., Gyöngyösi, A.Z., Breuer, H., Horváth, Á., Mona, T., and *Rajkai, K.*, 2014: Sensitivity of WRF-simulated planetary boundary layer height to land cover and soil changes. *Meteorol. Z. 23*, 279–293

Adams, S.M. and *Friedland, C.J.*, 2011: A survey of unmanned aerial vehicle (UAS) usage for imagery collection in disaster research and management." 9th International Workshop on Remote Sensing for Disaster Response.

Al-Harbi, K.M., 2001: Application of the AHP in project management. *Int. J. Proj. Manag. 19*, 19–27.

Balogh, M., Horányi, A., Gyöngyösi, A.Z., André, K., Mile, M, Weidinger, T., and *Tasnádi P.* 2011: The ALADIN/CHAPEAU model as a new tool for education and inter-comparison purposes at the Eötvös Loránd University in Budapest. *HIRLAM Newsletter 58*, November 2011.

Bankert, R. L. and *Hadjimichael, M.*, 2007: Data Mining Numerical Model Output for Single-Station Cloud-Ceiling Forecast Algorithms. *Weather Forecast. 22,* 1123–1131.

Bardossy A., Duckstein, L. and *Bogardi, I.*, 1993: Combination of fuzzy numbers representing expert opinions. *Fuzzy Set. Syst*. *57*, 173–181.

Bonin, T., Chilson, P., Zielke, B. and *Fedorovich, E.*, 2013: Observations of the Early Evening Boundary-Layer Transition Using a Small Unmanned Aerial System. *Bound.-Lay. Meteorol. 146*,119–132.

Bottyán, Z., Wantuch, F., Tuba, Z., Hadobács, K., and *Jámbor, K.*, 2012: Repülésmeteorológiai klíma adatbázis kialakítása az UAV–k komplex meteorológiai támogató rendszeréhez. *Repüléstudományi Közlemények 24*, 11–18. (In Hungarian.)

Bottyán, Z., Wantuch, F., Gyöngyösi, A.Z., Tuba, Z., Hadobács, K., Kardos, P., and *Kurunczi, R.*, 2013: Development of a Complex Meteorological Support System for UASs. *World Academy of Science, Engin. Technol. 7*, 648–653.

Breuer, H., Ács, F., Laza, B., Horváth, Á., Matyasovszky, I. and *Rajkai, K.*, 2005: Sensitivity of MM5-simulated planetary boundary layer height to soil dataset: comparison of soil and atmospheric effects. *Theor. Appl. Climatol. 109*, 577–590.

Bretherton, C.S. and *Park, S.*, 2009: A new moist turbulence parameterization in the Community Atmosphere Model. *J. Climate 22*, 3422–3448.

Büttner, G., Feranec, J., Jaffrain, G., Steenmans, C., Gheorghe, A., and *Lima, V.*, 2002: Corine land cover update 2000. Technical guidelines. Copenhagen, Denmark: European Environment Agency.

Chen, F. and *Dudhia, J.*, 2001: Coupling an advanced land-surface/hydrology model with the Penn State-NCAR MM5 modeling system, part I, Model implementation and sensitivity. *Month. Weather Rev. 129*, 569–585.

Cho, A., Kim, J., Lee, S. and *Kee, C.,* 2011:, Wind Estimation and Airspeed Calibration using a UAS with a Single-Antenna GPS Receiver and Pitot Tube. *Aerospace Electronic sys. 47*, 109–117.

Cuxart, J., Weidinger, T., Wrenger, B., Jimenez, M. A., Simo, G., Gomila, G., Warmers, H., Gyongyosi, A. Z., Istenes, Z., Bottyan, Z., Tatrai, D., Kiss, M., and *Jozsa, J.*, 2014: Joint Surface Budget Station, Tethered Balloon and RPAS Campaign SEABREEZE13 and PABLS13. ISARRA 2014 is held at Hans Christian Andersen Airport in Odense, Denmark, on May 26 to 28., http://www.isarra.org/isarra2014.html

Doswell III, C. A., Davies-Jones, R., and *Keller, D. L.*, 1990: On summary measures of skill in rare event forecasting based on contingency tables. *Weather Forecast. 5*, 576–585.

Drury, J.L., Riek, L. and *Rackliffe, N.,* 2006: A decomposition of UAS-related situation awareness. In proceedings of the 1st ACM SIGCHI/SIGART conference on Human-robot interaction, New York, NY, USA, 88–94.

Drüszler, Á; Vig, P. and *Csirmaz, K.*, 2011: Impacts of Hungarian Land Cover Changes on the Regional Climate during the 20th Century. In: XXVth Conference of the Danubian Countries, Budapest, Hungary.

Dudhia, J., 1989: Numerical study of convection observed during the Winter Monsoon Experiment using a mesoscale two-dimensional model. *J. Atmos. Sci. 46*, 3077–3107.

Evans, J.P., Ekström, M. and *Ji, F.*, 2012: Evaluating the performance of a WRF physics ensemble over South-East Australia. *Clim. Dynam. 39,* 1241–1258.

Fekete, Cs., and *Palik, M.*, 2012: Introduction of the Hungarian unmanned aerial vehicle operator's training course. *Def. Res. Manage. 21st Cent. 1*, 55–68.

Fövényi, A., 2010: Meteorológiai előrejelzések készítése sportrepülők részére numerikus modelladatok felhasználásával – régi és új módszerek adaptálása és automatizálása. *Repüléstudományi Közlemények 22* (Special Issue). (In Hungarian)

Garcia, M., Viguria, A., and *Ollero, A.*, 2013: Dynamic Graph-Search Algorithm for Global Path Planning in Presence of Hazardous Weather. Dynamic Graph-Search Algorithm for Global Path Planning in Presence of Hazardous Weather. *J. Intelligent Robotic Sys. 69*, 285–295.

Gertler, J., 2012: U.S. Unmanned Aerial Systems. Congressional Research Service. https://www.fas.org/sgp/crs/natsec/R42136.pdf.

Gyöngyösi, A.Z., Kardos, P., Kurunczi, R., and *Bottyán, Z.,* 2013: Development of a complex dynamical modeling system for the meteorological support of unmanned aerial operation in Hungary. Proceedings of International Conference on 28 – 31 May 2013, Atlanta, GA, USA.

Hansen, B., 2007: A Fuzzy Logic–Based Analog Forecasting System for Ceiling and Visibility. *Weather Forecast. 22*, 1319–1330

Hadobács, K., Tuba, Z., Wantuch, F., Bottyán, Z., and *Vidnyánszky, Z.*, 2013: A pilóta nélküli légijárművek meteorológiai támogató rendszerének kialakítása és alkalmazhatóságának bemutatása esettanulmányokon keresztül. *Repüléstudományi Közlemények 25*, 405–421. (in Hungarian)

Hágel, E., 2009: Development and operational application of a short-range ensemble prediction system based on the ALADIN limited area model. Ph.D. Thesis, Eötvös Loránd University, Faculty of Science.

Hirardelli, J.E.G., and *Glahn, B.*, 2010: The Meteorological Development Laboratory's Aviation Weather Prediction System. *Weather Forecast. 25*, 1027–1051.

Hong, S.-Y., Dudhia, J., and *Chen, S.-H.*, 2004: A Revised Approach to Ice Microphysical Processes for the Bulk Parameterization of Clouds and Precipitation. *Month. Weather Rev. 132*, 103–120.

Horányi, A., Mile, M., and *Szűcs, M.*, 2011: Latest developments around the ALADIN operational short-range ensemble prediction system in Hungary. *Tellus A 63*, 642–651.

Hu, X.-M., Nielsen-Gammon, J.W., and *Zhang, F.*, 2010: Evaluation of three planetary boundary layer schemes in the WRF model. *J. Appl. Meteorol. Climatol. 49*, 1831–1844.

Jacobs, A.J.M. and *Maat, N.,* 2005: Numerical guidance methods for decision support in aviation meteorological forecasting. *Weather Forecast. 20*, 82–100.

Kain, J. S., 2004: The Kain–Fritsch Convective Parameterization: An Update. *J. Appl. Meteorol. 43*, 170–181.

Marius, O.J, Ólafsson, H., Ágústsson, H., Rögnvaldsson, Ó., and *Reuder, J.*, 2012: Improving High-Resolution Numerical Weather Simulations by Assimilating Data from an Unmanned Aerial System. *Month. Weather Rev.140*, 3734–3756.

Martin, S., Bange, J. and *Beyrich, F.*, 2011: Meteorological profiling of the lower troposphere using the research UAS "M2AV Carolo". *Atmos. Measure. Tech. 4*, 705–716.

Meyer, M.A., Butterfield, K.B., Murray, W.S., Smith, R.E. and *Booker, J.M.*, 2002: Guidelines for eliciting expert judgment as probabilities or fuzzy logic. In (Eds.: *Ross, T.J., Booker, J.M.* and *Parkinson, W.J.*) Fuzzy Logic and Probability Applications: Bridging the gap. Society for Industrial and Applied Mathematics, 105–123.

Mikó, G., Kazi, K., Solymosi, J. and *Földes, J.*, 2009: UAS Development at BHE Bonn Hungary Ltd. 10th International Symposium of Hungarian Researchers on Computational Intelligence and Informatics, Proceedings. 2009, November 12-14, Budapest, Budapesti Műszaki Főiskola, 803–820.

Mireles, M., Kirth, R., Pederson, L. and *Elford, C. H.*, 2003: Meteorological Techniques (Revision 26 April 2006). No. AFWA/TN-98/002-REV. Air Force Weather Agency Offutt AFB NE.

Mlawer, E.J., Taubman, S.J., Brown, P.D., Iacono, M.J., and *Clough, S.A.*, 1997: Radiative transfer for inhomogeneous atmospheres: RRTM, a validated correlated k-model for the longwave. *J. Geophys. Res.: Atmos. 102(D14),* 16663–16682.

Murphy, A., H., 1992: Climatology, persistence, and their linear combination as standards of reference in skill scores. *Weather Forecast. 7,* 692–698.

Nurmi, P., 2003: Recommendations on the verification of local weather forecasts. The Library ECMWF Shinfield Park Reading, Berks RG2 9AX, 21 p.

Østbø, M., Osen P., Rokseth, G., Homleid O. V. and *Sevaldrud T.*, 2004: Exploiting meteorology toenhance the efficiency and safety of UAS operations. Forsvarets Forskningsinstitutt, Norwegian Defence Research Establishment FFI/RAPPORT-2004/00981, 50 p.

Passner, J.E., Dumais, R.E., Flanigan, Jr. R. and *Kirby, S.*, 2009: Using the Advanced Research Version of the Weather Research and Forecast Model in Support of ScanEagle Unmanned Aircraft System Test Flights. No. ARL-TR-4746, Computational and Information Sciences Directorate, ARL, 49 p.

Pásztor, L., Szabó, J. and *Bakacsi, Zs.*, 2010: Digital processing and upgrading of legacy data collected during the 1:25.000 scale Kreybig soil survey. *Acta Geodaetica et Geophysica Hungarica 45*, 127–136.

Restás, Á., 2013: On Half Way between the Military and Civil Use - Disaster Management Supported by UAS Applications. In (Eds. *Bale, P., Alderson, R.)* AUVSI 2013 Exhibition and Conference, Washington, USA, 2013. August 12-*15*, 1–10.

Restás, A. and *Dudás, Z.,* 2013: Some aspect of human features of the use of Unmanned Aerial Systems in a disaster-specific division International Conference on Unmanned Aircraft Systems. (ICUAS), 2013 28-31 May 2013 in Atlanta, GA, USA, DOI: 10.1109/ICUAS.2013.6564791.

Reuder, J., Brisset, P., Jonassen, M., Müller, M. and *Mayer, S.*, 2009: The Small Unmanned Meteorological Observer SUMO: A new tool for atmospheric boundary layer research. *Meteorol. Zeit.18,* 141–147.

Saaty, T.L., 1977: A scaling method for priorities in hierarchical structures. *J. Math.Psychol.15*, 234–281.

Saaty, T.L., 1991: Some mathematical concepts of analytic hierarchy process. *Behaviormetrika 29*, 1–9.

Seity Y., Brousseau P., Malardel S., Hello G., Bénard P., Bouttier F., Lac C., and *Masson V.*, 2011: The AROME-France Convective-Scale Operational Model. *Mon. Weather Rev. 139*, 976–999.

Skamarock, W.C., Klemp, J.B., Dudhia, J., Gill, D.O., Barker, D.M., Duda, M.G., Huang, X-Y., Wang, W. and *Powers, J.G.*, 2008: A description of the Advanced Research WRF Version 3. NCAR/TN-475 + STR NCAR Technical Note.

Somlyai, L., Turóczi, A. and *Molnár, A.*, 2012: Atmospheric analyser for mobile robots. *Computational* Intelligence and Informatics (CINTI), 2012 IEEE 13th International Symposium on Date 20–22 November, 2012 Budapest.

Souders, C.G. and *Showalter, R.C.*, 2008: Transformation of NAS to NEXTGEN and FAA's weather architecture impacts: an update. Aerospace Meteorology, AMS 88th Annual Meeting.

Sousounis, P.J., 2005: Short term turbulence forecasts over the Atlantic Ocean using WRF. Preprints, World Weather Research Program Symposium on Nowcasting and Very Short Range Forecasting, September 5-9 2005. Toulouse, France.

Stenmark, A., Hole, L.R., Voss, P., Reuder, J. and *Jonassen, . M.O.*, 2014: The Influence of Nunataks on Atmospheric Boundary Layer Convection During Summer in Dronning Maud Land, Antarctica." *J. Geophys.Res. Atmospheres 119* (11) 6537–6548.

Sun, X., Cai, C. and *Shen, X.*, 2014: A New Cloud Model Based Human-Machine Cooperative Path Planning Method. *J. Intelligent Robotic Sys.*

Szabó, Z. A., 2014: Pilóta nélküli repülőgépeken alkalmazható szondázási módszerek vizsgálata és fejlesztése. MSc Thesis, Department of Meteorology Eötvös Loránd University (In Hungarian).

Szabó, Z.A., Istenes, Z., Gyöngyösi, A.Z., Bottyán, Zs., Weidinger, T. and *Balczó, M.*, 2013: Sounding the planetary boundary layer with Unmanned Aerial Vehicles (UAS). *Repüléstudományi Közlemények 25,* 422–434. (In Hungarian.)

Toth, Z., 1989: Long-Range Weather Forecasting Using an Analog Approach. *J.Climate 2*, 594–607.

Tuba, Z., Bottyán Z., Wantuch, F. Vidnyánszky, Z. and *Hadobács K.*, 2013a: Meteorological support model for meteorological support in military mission planning. *Hadmérnök 8*, 294–304. (in Hungarian)

Tuba, Z., Vidnyánszky, Z., Bottyán, Z., Wantuch, F. and *Hadobács, K.*, 2013b: Application of Analytic Hierarchy Process (AHP) in fuzzy logic-based meteorological support system of unmanned aerial vehicles. *Acad. Appl. Res. Military Sci. 12*, 221–228.

Tuba, Z., 2014: Selected questions of Unmanned Aerial Vehicles (UASs) and visibility. *Repüléstudományi Közlemények 26*, 94–105. (in Hungarian)

Varga, Á. and *Balczó, M.*, 2013: Development of a multi-hole probe for atmospheric boundary layer Measurements. PHYSMOD 2013 – International Workshop on Physical Modeling of Flow and Dispersion Phenomena EnFlo Laboratory, University of Surrey, UK, 16th – 18 th September 2013. http://www.dapple.org.uk/Physmod.html

Wang, W., Bruyère, C., Duda, M. G., Dudhia, J., Gill, D., Lin, H. C., Michalakes, J., Rizvi, S. and *Zhang, X.*, 2009: WRF-ARW Version 3 Modeling System User's Guide, July 2009, Mesoscale & Microscale Meteorology Division, National Center for Atmospheric Research, Boulder, USA Tech. Note.

Wantuch, F., 2001: Visibility and fog forecasting based on decision tree method. *Időjárás 105*, 29–38.

Wantuch, F., Bottyán, Z., Tuba, Z. and *Hadobács, K.*, 2013: Statistical Methods and Weather Based Decision Making in Meteorological Support for Unmanned Aerial Vehicles (UASs). Proceedings of International Conference on 28 – 31 May 2013, Atlanta, GA, USA.

Watts, A.C., Ambrosia, W.G. and *Hinkley, E.A.,* 2012: Unmanned Aircraft Systems in Remote Sensing and Scientific Research: Classification and Considerations of Use. *Remote Sensing 4*, 1671–1692.

Weidinger, T., Cuxart, J., Gyongyosi, A.Z., Wrenger, B., Istenes, Z., Bottyan, Z., Simó, G., Tatrai, D., Jericevic, A., Matjacic, B., Kiss, M. and *Jozsa, J.*, 2014: An experimental and numerical study of the ABL structure in the Pannonian plain (PABLS13). AMS, 21st Symposium on Boundary Layers and Turbulence. June 09 - 13, 2014, Leeds, United Kingdom. ams.confex.com/ams/21BLT/webprogram/21BLT.html

Williams, K.W., 2004: A Summary of Unmanned Aircraft Accident/Incident Data: Human Factors Implications. Final report, Federal Aviation Administration Oklahoma City Ok Civil Aeromedical Inst., ADA460102, 17 p.